Density fluctuations in a model for vibrated granular media

Mario Nicodemi,[1,2] Antonio Coniglio,[1,2] and Hans J. Herrmann[1,3]
[1]*PMMH ESPCI, 10 rue Vauquelin, 75231 Paris Cedex 05, France*
[2]*Dipartimento di Scienze Fisiche, Università di Napoli ''Federico II,'' INFM and INFN Sezione di Napoli, Mostra d'Oltremare, Padiglione 19, 80125 Napoli, Italy*
[3]*ICA 1, Universität Stuttgart, Pfaffenwaldring 27, 70569 Stuttgart, Germany*
(Received 2 June 1997; revised manuscript received 4 November 1998)

This paper presents the study of density fluctuations in a model for vibrated granular media. Their microscopic origin is shown to be linked to the microscopic disorder in grains packing. Varying vibrations amplitude and duration, several regimes are found for density relaxation. Its power spectrum is well described by power laws. [S1063-651X(99)16905-8]

PACS number(s): 81.05.Rm, 05.40.−a, 45.05.+x, 81.20.Ev

I. INTRODUCTION

The problem of density fluctuations in vibrated granular media has large importance in many practical applications and opens questions from more fundamental points of view [1,2]. Strong fluctuations are commonly observed in these materials for instance in the measures of contact forces [3], of stress in sheared [4] or flowing [5] or compressed [6] granular media, during density compaction [7–9], in the density of granular systems flowing during the discharge from bins or pipes [10–12], and actually their strength makes a systematic study a nontrivial task. Here we try to show how strong fluctuations in ''dynamical'' processes, as density compaction under taping, are related to microscopic mechanisms as geometric disorder and frustration present in granular packs.

Several models have been proposed to describe the dynamics of a dense granular material as nonlinear master equations [8,13–15] or Monte Carlo simulations which introduce *ab initio* frustration due to the hard-core interaction between the grains [16–18] (see also [1]). Recently a simple microscopic model was introduced [19] to elucidate the role that disorder in particle arrangements, typical of granular media, plays in such systems. This model, which can be mapped into an Ising spin glass, is a lattice gas whose particles, subjected to gravity and vibrations, have to satisfy during their motion the local geometrical constraints due to the nontrivial neighbors arrangement. Interestingly it shows highly nontrivial dynamic features, as logarithmic compaction or segregation [19], in strict correspondences with experimental facts about granular assemblies. In this context we face the problem of a systematic analysis of density fluctuations during tapping which may be compared with experimental observations of vibrated dry granular media in the low amplitude regime. The model allows to sketch a microscopic detailed picture of the phenomenon and to predict several characteristic properties to be experimentally verified.

This analysis shows that density relaxation presents fluctuations of the same order of magnitude of the measured mean values. In particular the power spectrum of the density relaxations, $S(\omega)$, presents several regions as a function of the frequency. $S(\omega)$ goes to a constant at very small frequencies; then an intermediate region with a power law behavior is found; and, at even higher frequencies, we observe a more usual behavior which corresponds to short time exponential-like relaxations. The intermediate region may be a wide nontrivial portion of the spectrum, but it seems to always present a finite upper cut off. Power law behaviors have been typically found in granular media [1,2], and our general results seem well consistent with the known experimental data for density compaction [7–9].

II. LATTICE MODEL

As stated, the model introduced in [19], which we study here, was conceived to take into account the effects of disorder and geometrical frustration in particle rearrangements typically present in granular media. It is essentially a lattice gas whose particles have to fulfill local geometrical constraints, which, in the present version, are ''quenched'' on the lattice (see [20] for a model without quenched disorder, where we expect behaviors similar to those discussed here). For the sake of clarity we briefly summarize its main features. The model consists of a system of particles diffusing on a square lattice (a three-dimensional version of the model is studied in Ref. [21]). On site i we set $n_i=1$ if a particle is present and 0 otherwise. Moreover, the particles are characterized by an internal degree of freedom $S_i=\pm 1$ (an Ising spin), describing local quantities, as particles shape orientation, which actually experience geometrical frustration [19]. $S_i=1$ might correspond to a rodlike shaped grain whose elongation is directed along one lattice direction and $S_i=-1$ to a grain oriented in the other direction.

In real granular media, grains are typically frustrated in their motion and packing, by several microscopic mechanisms as, for instance, geometrical effects due to hard core repulsion with their neighbors or friction phenomena. Moreover, a high degree of disorder is typically present in the packs. In the present model we describe these facts by assigning fixed random numbers, $\epsilon_{ij}=\pm 1$, to the bonds of the lattice. The bond variables ϵ_{ij} schematically model the general effects of the disorder of the environment and geometric frustration present in granular systems due to spatial mismatch of grains shapes and arrangements disregarding the actual mechanisms from which they arise. Our results are

linked to these general aspects of the model and are essentially independent of their specific realization (see also [19–21]). In the present model particles are subjected to the constraint to fit the local ''geometrical'' arrangement imposing that whenever two (i and j) are neighboring, their ''orientation'' must satisfy the mutual and the environmental geometrical disposition according the following relation: $\epsilon_{ij}S_iS_j=1$. Particles react to the effects of the ''quenched'' frustration imposed by the choice of the ϵ_{ij}, which leads to the unavoidable presence of empty sites. It is possible to give a formulation of such a model [22,23,19] in terms of an Edwards-Anderson Ising spin glasslike Hamiltonian [24].

We are interested in studying such a system when undergoing a dynamical processes in the presence of ''external vibrations'' and ''gravity.'' So we define a dynamics based on the random diffusion of particles on a square lattice whose diagonal is parallel to the direction of gravity, in such a way as to preserve the above ''geometrical'' constraints. When just gravity is present, particles may just move down, while in the presence of shaking they can also be pushed up. Thus, the particles attempt a move upwards with probability P_2 and downward with $P_1(P_1+P_2=1)$. The move is made only if the internal degrees of freedom satisfy the above constraint and if the place is empty. Similarly, their orientation S_i (the ''spin'') may randomly flip if there is no violation of constraints, and does not flip otherwise. In the absence of vibrations, the presence of gravity imposes $P_2=0$. When vibrations are switched on, P_2 becomes finite. The single parameter that controls the dynamics and describes the vibrations is the ratio $x(t)=P_2(t)/P_1(t)$. As described in more detail in Refs. [19–21], the parameter x is linked to an ''effective temperature,'' β^{-1}, of the system $\beta=-\ln(x)$, and is thus related to the adimensional experimental shaking amplitude Γ (see [1]).

We adopt, for our Monte Carlo simulations, a 45° tilted lattice with periodic boundary conditions along the horizontal axis (respect to gravity) and rigid walls at bottom and top. Further results about three-dimensional systems [21] show the generality of our finding in two dimensions. After fixing the random quenched ϵ_{ij} on the bonds, a random initial particle configuration is prepared by randomly pouring particles into the box from its top and then letting them fall down, with the described dynamics ($P_2=0$).

III. MONTE CARLO RESULTS

Our aim is the study of density fluctuations during compaction in the presence of vibrations. As in real experiments we consider dynamical processes consisting of sequences of taps. A ''tap'' in a real experiment is the shaking of a container filled with grains by vibrations of given duration and amplitude. In our Monte Carlo simulations each tap is defined by giving a finite value to the dynamic parameter x. Specifically we fix $x(t)=x_0=\text{const}$ for $t\in[0,\tau]$ and later $x_0=0$. With this procedure the systems attains, after ''shaking,'' a final ''static'' configuration that is defined by the criterion that during a fixed time t_r nothing changes any longer. We fixed in our simulation $t_r=330$, much longer than any other characteristic time in the system (at $x_0=0$). Time t is measured in such a way that one unit corresponds to one single average update of all particles and spins of the lattice. We interpret τ as the duration of the vibrations and x_0 as their amplitude. After each tap we measure the static bulk density of the system $\rho(t_n)$(t_n is the nth tap number), i.e., the density in the lower 25% of the box. We repeat the tapping sequence for different values of the tap amplitude x_0 and fixed duration τ.

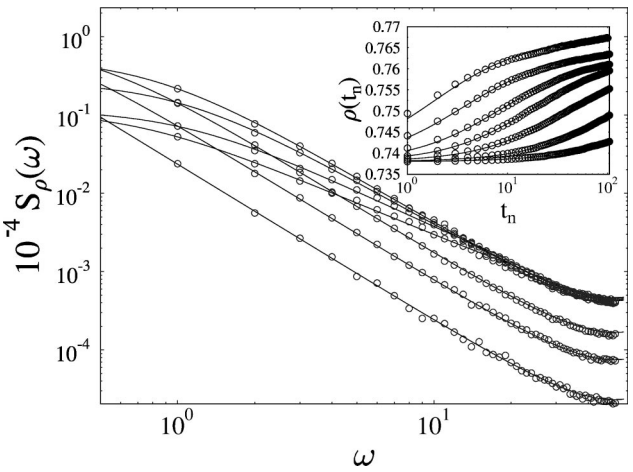

FIG. 1. Power spectrum, $S_\rho(\omega)$, of MC data for density relaxation as a function of the frequency number ω, for sequences of taps of vibration amplitude $x_0=2.0\times10^{-4}$, 5.0×10^{-4}, 2.0×10^{-3}, 5.0×10^{-3}, 1.0×10^{-2},2.0×10^{-2},0.1 (from bottom to top) and duration $\tau=37$. The continuous curves are power law fits described in the text [Eq. (7)] whose parameters are shown in Fig. 5. Inset: Static bulk density $\rho(t_n)$ from the same MC data described (from bottom to top) above as a function of tap number t_n. The continuous curves are inverse logarithmic fits, given in the text [Eq. (1)], proposed to interpolate experimental data, whose parameters are given in Fig. 2.

For this Monte Carlo experiment, which requires very long computer time, we considered a system of size 30×60. Our data are averaged over 640 different ϵ_{ij} configurations to produce highly reliable data. The drawback was that we were unable to make simulations for very long tapping sequences: we generally fix to 100 the total number of taps in a sequence. However, as explained below, we also made test runs with less good statistics but longer time series (one order of magnitude more) to verify that our results are valid (see also Fig. 6). A test of size effects was also performed, where larger systems were studied (up to size of 100×200, see also [19]). This analysis allows us to conclude that our results are very robust to size effects. However, the phenomenon of density relaxation is logarithmic in t_n; thus, generally speaking, we cannot exclude that our analysis (with t_n up to 10^3) is not valid in the truly asymptotic time regime.

A. Density relaxation under tapping

To describe experimental observations about grain density compaction under a sequence of taps an inverse logarithmic law was actually proposed in Ref. [7]. In the present model, data of density relaxation proved to satisfy the same law [19]. In the inset of Fig. 1 we show our Monte Carlo data for the density relaxation during a sequence of taps for several values of the vibration amplitude x_0. The superimposed fits are from the logarithmic law presented in [7], cast in the following form:

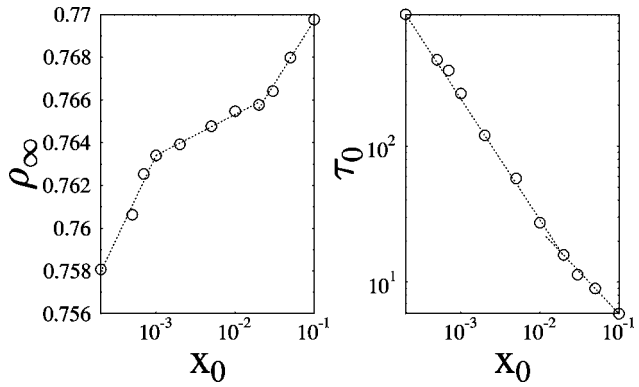

FIG. 2. Fit parameters ρ_∞ and τ_0 for density relaxation (data of Fig. 1), from the inverse logarithmic law, given in the text, Eq. (1), as a function of the tap vibration amplitude x_0. The behavior of ρ_∞ shows the appearance of three approximate rough regions separated by $x_1^* \sim 10^{-3}$ and $x_2^* \sim 10^{-2}$. The characteristic time of logarithmic relaxations, $\tau_0(x_0)$, can be described by two power laws.

$$[\rho(t_n)-\rho_\infty]/(\rho_0-\rho_\infty)=\ln(c)/\ln(t_n/\tau_0+c). \qquad (1)$$

Here ρ_∞ is the final asymptotic density and ρ_0 its initial measured value. Notice that one can fit the very long time data of density compaction under tapping also with a stretched exponential four parameter function, which, at high x_0 values performs as well as the above inverse logarithm. However, with the logarithm one is able to fit the full set of data (not just long times) for all the explored values of x_0.

We present here results for the fits of our data with Eq. (1) on which we imposed the constraint that the fit function passes at $t_n=0$ through $\rho_0=0.739$, i.e., the measured static initial state density of our system obtained from the prepared random starting configuration (in which the particles were poured into the box according to the rules given above). We found that for the sequences of our MC taps of fixed duration τ and amplitude x_0, the parameter c of Eq. (1) is approximately equal to $c=1.3$ and independent of x_0 in the explored amplitude $x_0 \in [2.0\times10^{-4},0.1]$ and duration range $\tau \in [0.037,370]$. The phenomenological parameter c may be linked to a second typical time, other than τ_0, in the system.

The two parameters ρ_∞ and τ_0 obtained by fitting with Eq. (1) our MC data for sequences with fixed tap $\tau=37$ and tap ''amplitude'' $x_0 \in [2.0\times10^{-4},1.0\times10^{-1}]$, are reported in Fig. 2. Consistent with what was found experimentally in Ref. [7], and in agreement with some previous results [19], the characteristic time τ_0 diverges when the vibrations amplitude goes to zero with a power law in x_0 (at low vibration amplitudes and at fixed $\tau=37$),

$$\tau_0(x_0)=(x_0/X)^{-\gamma}. \qquad (2)$$

In the very low amplitude region the exponent is $\gamma=0.9$ and $X=0.4$, but the data show a crossover to $\gamma=0.6$ and $X=1.8$ above $x_2^* \approx 10^{-2}$. As a function of the effective temperature, β^{-1}, τ_0 should then follow an Arrhenius law. The other parameter ρ_∞ shows a more complex behavior with x_0. Approximately three rough regimes seem to appear characterized by two typical amplitude values: x_2^* and $x_1^* \approx 10^{-3}$. A possible approximate fit in these regions of intermediate values of x_0 is

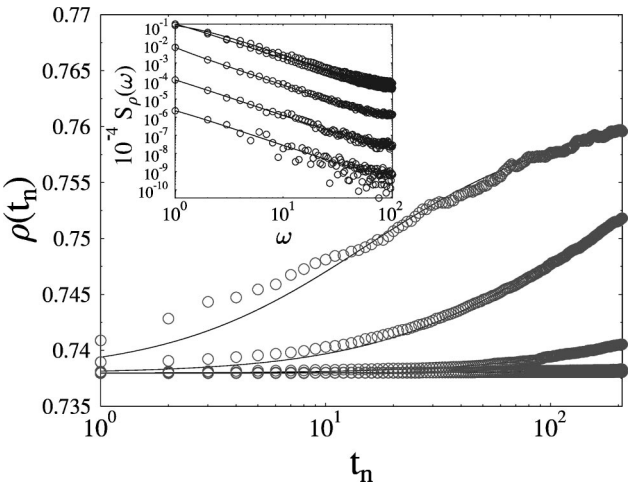

FIG. 3. Static bulk density $\rho(t_n)$ from our MC data as a function of tap number t_n, for tapping sequences of fixed vibration amplitude $x_0=5.0\times10^{-4}$ and duration $\tau=0.037,0.37,3.7,37,370$ (from bottom to top). The continuous curves are the quoted logarithmic fits, whose parameters are shown in Fig. 4. In the inset we show the corresponding power spectrum (analogous to the spectrum of the data of Fig. 1) with the power law fits described in the text whose parameters are shown in Fig. 4.

$$\rho_\infty(x_0)=r_1+r_0\log(x_0), \qquad (3)$$

with $r_1=0.79$, $r_0=0.003$ below x_1^*, $r_1=0.75$, $r_0=0.001$ between x_1^* and x_2^*, and $r_1=0.77$, $r_0=0.002$ above x_2^*.

We also analyzed the dependence of these laws and parameters by changing the tap ''duration'' τ. We simulated tapping sequences of 200 taps with fixed $x_0=0.0005$ and $\tau=0.037,0.37,3.7,37,370$. The data from these sequences, averaged over 320 ϵ_{ij} configurations, are depicted in Fig. 3. We find again the logarithmic behavior given in Eq. (1), in which approximately $c=1.3$. The other two parameters, ρ_∞ and τ_0, are given in Fig. 4 as a function of τ. As above we find that they are well described by power laws,

$$\tau_0(\tau)=(\tau/A)^{-\gamma'}, \qquad (4)$$

with $A=1.1\times10^4$ and $\gamma'=0.9$ in agreement with the previous value for γ of Eq. (2) in the low vibration amplitudes region. As expected the characteristic time τ_0 diverges when either $x_0 \to 0$ or $\tau \to 0$. For small vibration amplitudes or durations, the asymptotic density ρ_∞ increases with x_0 and τ. As above, we fit the data approximately with

$$\rho_\infty(\tau)=r_3+r_2\log(\tau), \qquad (5)$$

with $r_3=0.75$, $r_2=0.003$.

B. Power spectrum of density relaxation

A further characterization of our time series for density relaxation is obtained by studying their spectral properties and fluctuations. As usual, we define the power spectrum $S_\rho(\omega)$ of our density sequences $\rho(t_n)$ (with $t_n \in \{0,T\}$, where T is the total number of taps, which in our case is typically $T=100,1000$), as

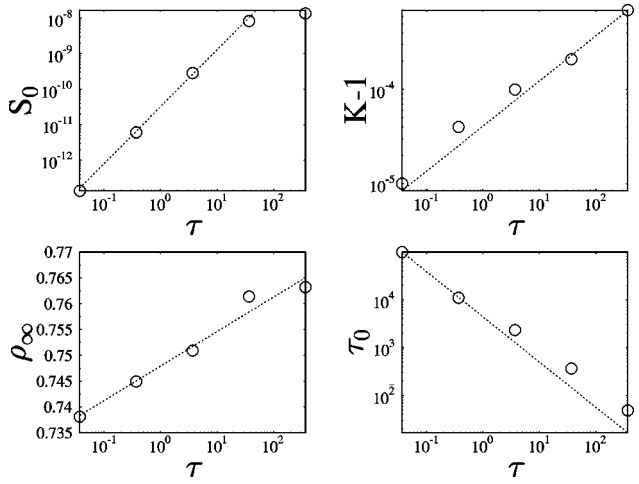

FIG. 4. Lower figures: fit parameters of logarithmic law, ρ_∞ and τ_0, for density relaxation in the sequences of taps shown in Fig. 3 of fixed amplitude $x_0=5.0\times10^{-4}$ and duration $\tau=0.037,0.37,3.7,37,370$, as a function of τ. Upper figures: fit parameters $S_0,\omega_0(\xi\simeq1)$, for power law density spectrum $S_\rho(\omega)$ in the low frequencies region, as a function of the frequency number ω, for the same sequences described above. These behaviors are similar to those found for the other kind of tap sequences (fixed duration τ and varying amplitude x_0) shown in Fig. 1.

$$S_\rho(\omega)=\left|\frac{1}{T}\sum_{t_n=1,T}\rho(t_n)\exp\left(\frac{2\pi i}{T}t_n\omega\right)\right|^2, \tag{6}$$

where $\omega\in\{0,1,\ldots,T/2\}$ is an integer.

Being that the density relaxation is approximately logarithmic, it is problematic to decide where one enters the asymptotic ''stationary'' regime. We thus study the spectral properties of the full relaxation to compare it with experimental data.

The typical appearance of the spectrum $S_\rho(\omega)$ as a function of ω is shown in Fig. 1 for our series of taps of fixed duration $\tau=37$ and the quoted values of ''amplitudes'' x_0, described at the beginning of Sec. III A. We approximately find the following regions: a saturation to a constant $S_\rho(\omega)\sim S(0)$, as a ''white noise'' behavior, at very small frequencies; then up to a frequency ω_1 a power law with an eventually nontrivial exponent $\xi\leqslant1$, $S_\rho(\omega)\sim\omega^{-2\xi}$; and, for high frequencies, a more usual behavior corresponding to short time exponential relaxations. Interesting is the behavior at low vibration amplitude. Actually when $x_0\to0$, we find also below ω_1 that $\xi=1$. So a frequency region is present whose extensions are larger the smaller x_0, where trivial power laws are observed, corresponding, as stated, to a short time exponential-like behavior. Moreover, the portion of the spectrum with $\xi\leqslant1$ always has a finite upper cutoff ω_1, above which we find $\xi=1$.

The spectrum from our MC density series (for the same amplitude range $x_0\in[2.0\times10^{-4},0.1]$ and duration $\tau=37$ reported above) is depicted in Fig. 1. Our data may be generally well fitted by power laws as the following:

$$S_\rho(\omega)=S_0\left[K-\cos\left(\frac{2\pi\omega}{T}\right)\right]^{-\xi}. \tag{7}$$

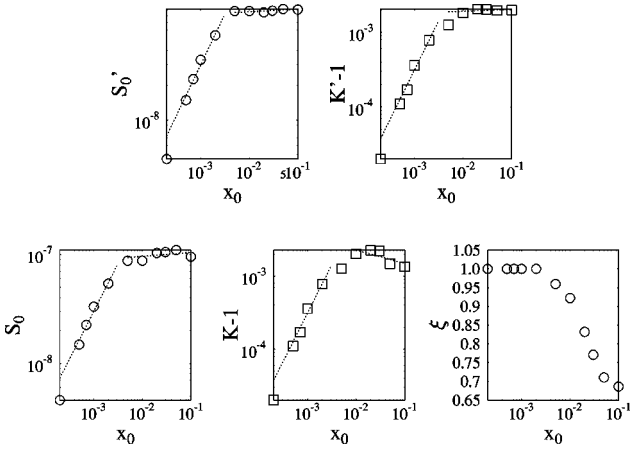

FIG. 5. Lower figures: fit parameters S_0,ω_0,ξ of the density spectrum $S_\rho(\omega)$ in the low frequencies region ($\omega<\omega_1=T/4$, where $T=100$ is the total number of taps in the sequences), as a function of the vibration amplitude x_0 at fixed $\tau=37$ (τ is the duration of a single tap) for the same data shown in Fig. 1. Superimposed curves are the power law fit described in the text. Upper figures: fit parameters S_0' and $K'-1$ for $S_\rho(\omega)$ in the frequencies zone above ω_1.

This law, when $\xi=1$, is the spectrum, via discrete Fourier transform, of a standard exponential function.

For our fits we divided the data in two frequency regions. Above a frequency $\omega_1\sim T/4$ (actually ω_1 is a function of x_0) we always find $\xi=1$. This suggests that at very small tap number density compaction follows a usual exponential-like behavior as found in the model of Ref. [17]. The parameters S_0 and $K-1$ of the fit with Eq. (7) of MC data in the region $\omega>\omega_1$, are reported in the top row of Fig. 5. We find that above x_2^* they are almost independent of x_0.

The behavior with $\xi=1$, at low vibration amplitude, extends over the whole frequency region we reached, also above ω_1. However, the scenario changes above a vibrations amplitude approximately equal to x_1^*, where a low frequency portion of the spectrum appears in which the exponent ξ is well below 1. The fit of this part of the spectrum below ω_1 is still done with Eq. (7), and the fit parameters of MC data are depicted in the bottom part of Fig. 5. The observations of the previous section about the power law behavior of τ_0 as a function of x_0 suggest an analogous behavior for the characteristic frequency $\omega_0\equiv(K-1)^{1/2}$ of Eq. (7). We find two regimes as a function of x_0, approximately separated, as above, by the value x_2^*. Below x_2^*,

$$\omega_0(x_0)^2\equiv(K-1)=(x_0/Y)^\alpha, \tag{8}$$

with $\alpha=1.6$ and $Y=0.4$, and, above x_2^* $K-1$ is approximately constant ($K-1\sim1.5\times10^{-3}$). The exponent ξ is equal to 1 up to x_1^* and then apparently decreases, as shown in Fig. 5.

Also S_0 has approximately a power law behavior divided in two regions separated by the same value x_2^*,

$$S_0(x_0)=(x_0/Z)^\delta, \tag{9}$$

where $\delta=0.9$ and $Z=0.41$ below x_2^* and $S_0\sim0.01$ constant above.

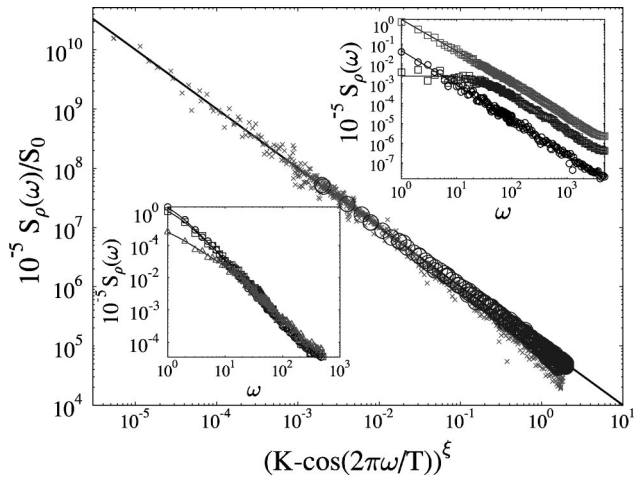

FIG. 6. Inset (top right): density relaxation power spectrum $S_\rho(\omega)$ from experimental data recorded by Knight *et al.* (see text) for several values of the adimensional tap amplitude Γ ($\Gamma = 1.4,2.3,2.7$, from bottom to top). $\Gamma = a/g$ is the ratio of the peak acceleration, a, of a tap to $g = 9.81$ m/s^2, the gravitational acceleration. Continuous curves are fits with the power law, Eq. (7), quoted in the text, whose exponent is respectively $\xi = 0.87,0.77,0.79$. Main frame: the above experimental data from Knight *et al.* (crosses) and our MC data shown in Fig. 1 (circles) about power spectrum of density relaxation, $S_\rho(\omega)$, as a function of the frequency number ω, rescaled according to the function given in the text, Eq. (7). Inset (bottom-left): Power spectrum of MC data on density relaxation $S_\rho(\omega)$ as a function of the frequency number ω, for sequences of taps with vibrations of amplitude $x_0 = 5.0 \times 10^{-3}, 1.0 \times 10^{-2}, 1.0 \times 10^{-1}$ and duration $\tau = 37$. These MC sequences are depicted to show the consistency with the results from the shorter sequences (one order of magnitude less) with better statistic shown in Fig. 1.

We tested that our general results are not affected by the duration of our time series $T = 100$, by recording the same behaviors for a longer tap sequence with $T = 1000$ but lower statistics. The findings, reported in the inset in the bottom of Fig. 6, confirm our previous results.

These general results are consistent with the experimental data known to us. To compare our results with experiments, we show in the top inset of Fig. 6 the spectrum $S_\rho(\omega)$ from experimental measurements made by Knight *et al.* [7]. The experimental data of Knight *et al.* on grain density compaction concern the measure taken at the bottom of a shaken box for $\Gamma = 1.4,2.3,2.7$, where Γ is the ratio of the peak acceleration of a tap, a, to $g = 9.81$ m/s^2, the gravitational acceleration ($\Gamma = a/g$). To show the direct correspondence between our MC data and experimental data, we report in the main frame of Fig. 6 (as a single picture) the spectrum from our series at different vibration amplitudes (shown in Fig. 1) and those from the measurements by Knight *et al.* [7] both rescaled according Eq. (7). Each data set is rescaled with its value of the fit parameter ξ measured in the low frequency region (the values of $\xi = 0.87,0.77,0.79$ for the quoted experimental data are in the same range of our MC). The scaling seems to work well over several orders of magnitude of the rescaled variable, except for the high frequency data ($\omega > \omega_1$), where both experimental measures and our MC have, as explained above, a different exponent $\xi = 1$.

We repeated the same analysis for the sequences with tap duration $\tau = 0.037,0.37,3.7,37,370$ and fixed amplitude $x_0 = 0.0005$. The picture outlined above doesn't change and the spectrum, described by Eq. (7), is reported in the inset of Fig. 3. The parameters defined in Eq. (7), depicted in Fig. 4, again seem to follow power laws,

$$\omega_0(\tau) \equiv K - 1 = (\tau/C)^{\alpha'}, \tag{10}$$

where $\alpha' \simeq 0.5$ and $C \simeq 2.1 \times 10^9$, and

$$S_0(\tau) = (\tau/D)^{\delta'}, \tag{11}$$

where $\delta' \simeq 1.4$ and $D \simeq 3.6 \times 10^2$. In the present case, working at very low amplitude and small durations of the taps, we always find that the exponent ξ is approximately equal to 1. At low x_0 we are unable to enter the zone of the power spectrum with $\xi < 1$.

As a consequence of the above results, when $x_0 \to 0$ or $\tau \to 0$, we expect that the power spectrum $S_\rho(\omega)$ obeys the following trivial scaling relation with vibration amplitude x_0 (or analogously with τ):

$$S_\rho(\omega; x_0) = x_0^\delta f_T(\omega/x_0^\alpha), \tag{12}$$

where $f_T(y)$ is a universal scaling function. This equation is, however, not expected to be valid in the low frequency regions where ξ may no longer be equal to 1.

C. Density fluctuations

We pass now to a brief discussion of higher moments of density series measurements. Specifically we analyze the relative density fluctuations $\sigma(t_n)$ around the measured mean value $\rho(t_n)$ and the fourth order cumulant $g(t_n)$ to extract informations about its distribution. We study the quantities σ and g defined as

$$\sigma(t_n) = \left[\frac{\langle \rho^2(t_n) \rangle - \langle \rho(t_n) \rangle^2}{\langle \rho(t_n) \rangle^2} \right]^{1/2}, \tag{13}$$

$$g(t_n) = \frac{1}{2} \left[3 - \frac{\langle \rho^4(t_n) \rangle}{\langle \rho^2(t_n) \rangle^2} \right], \tag{14}$$

where the averages run over the quoted 640 different realizations.

Like the density ρ, σ also follows an inverse logarithmic law similar to the one given in Eq. (1),

$$\sigma(t_n) = \sigma_\infty - \Delta\sigma / \ln(t_n/\tau_\sigma + c), \tag{15}$$

where c is still fixed to 1.3. Our results are reported in Fig. 7 for the same series of values of x_0 described above in Sec. III A with $\tau = 37$. We note that the fluctuation are of the same order of the density itself ($\sigma \sim 1$) and that they are stronger and more persistent at lower vibration amplitudes. The times τ_σ of Eq. (15) are, within a 10% error, equal to those found for τ_0 in Eq. (1). $\Delta\sigma \sim 0.28 \pm 0.02$ is approximately constant. Also the study of σ_∞, depicted in Fig. 7, hardly shows the three regions found for the parameters of Eq. (1). This may be due to the poorer data quality we obtain for higher moments.

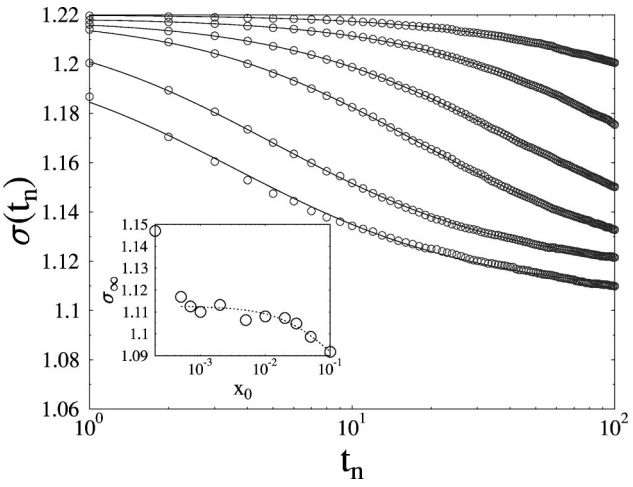

FIG. 7. Relative density fluctuations from MC data, $\sigma(t_n)$, as a function of the logarithm of the tap number t_n, for the same tapping series of Fig. 1 with vibrations of amplitude $x_0=2.0\times10^{-4}$,5.0×10^{-4}, 2.0×10^{-3},5.0×10^{-3}, 1.0×10^{-2},2.0×10^{-2} (from top to bottom) and duration $\tau=37$. The continuous curves are fits with the inverse logarithmic function described in the text. Inset: the estimated asymptotic value, σ_∞, for density fluctuations $\sigma(t_n)$, as function of the vibration amplitude x_0.

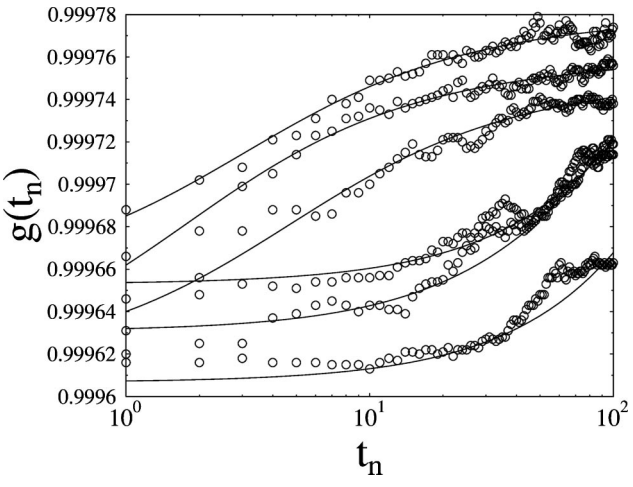

FIG. 8. Fourth order cumulant of density fluctuations from MC data, $g(t_n)$, as a function of the logarithm of the tap number t_n, for the same tapping series of Fig. 1 with vibrations of amplitude $x_0=2.0\times10^{-4}$, 5.0×10^{-4}, 2.0×10^{-3}, 5.0×10^{-3}, 1.0×10^{-2}, 2.0×10^{-2} (from bottom to top) and duration $\tau=37$. The continuous curves are inverse logarithmic fits.

The quality of our data is even poorer for g, which is depicted in Fig. 8 for the same series of values of x_0 described above. Note the fine scale of the ordinate, $g\in[0.999\ 61,0.999\ 78]$: this implies that the fourth moment of the distribution of measures is essentially equal to the second. Also in this case a fit with Eq. (15) is reasonable, but the fit parameters fluctuate much more. However, the characteristic times of the logarithmic fits show the same behavior found above for τ_0 and τ_σ [actually the simple moments $\rho(t_n)$, $\rho^2(t_n)$ and $\rho^4(t_n)$ have all the same time scales]. These fit parameters are shown in Fig. 9.

All these findings may be resumed by stating that the mean square fluctuations observed in the measure of density are typically of the same order of magnitude of the average itself. The relative fluctuations are stronger at lower vibration amplitude. The fourth moment is of the same order of the second. Moreover, their dependence on the tap number t_n follows the same inverse logarithmic law given, for the density, in Eq. (1).

D. Density correlation function

We have also recorded the density time correlation function, $C(t_n)$, defined as

$$C(t_n)=\frac{\langle\rho(t_n)\rho(t_1)\rangle-\langle\rho(t_1)\rangle^2}{\langle\rho^2(t_1)\rangle-\langle\rho(t_1)\rangle^2}. \tag{16}$$

As above, the time correlation function $C(t_n)$ has an inverse logarithmic behavior given, for instance, in Eq. (1), again with $c=1.3$. In this case, of course, we have the additional constraint that the curves have to pass through 1 at $t_n=1$. Our results for the quoted values of x_0 are reported in Fig. 10.

Also now the times of this logarithmic relaxation are, within a 10%, consistent with the corresponding values found for τ_0 in Eq. (1). In the inset of Fig. 10 we plot the asymptotic estimated value c_∞ of the correlation function $C(t_n)$ for the studied values of x_0 [$c_\infty=\lim_{t_n\to\infty}C(t_n)$]. We just note that c_∞ is well above zero in the full interval of x_0 studied.

Consistent with the previous results, the power spectrum $S_C(\omega)$ of the correlation function $C(t_n)$ shows a behavior very similar to that described above in some detail for $S_\rho(\omega)$ [analogously for $\sigma(t_n)$ and $g(t_n)$]. Equation (7) seems to be satisfied and its parameters approximately follow Eqs. (8) and (9) as a function of vibration amplitude x_0. The statistics for $S_C(t_n)$ is worse than that for S_ρ, and the data less clear.

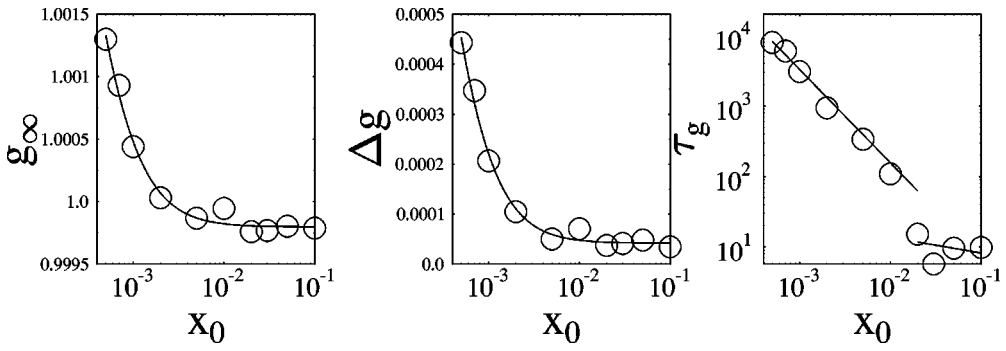

FIG. 9. The parameters g_∞, Δg, and τ_g from the logarithmic fit of the fourth order cumulant, $g(t_n)$ (shown in Fig. 8), as a function of the vibration amplitude x_0.

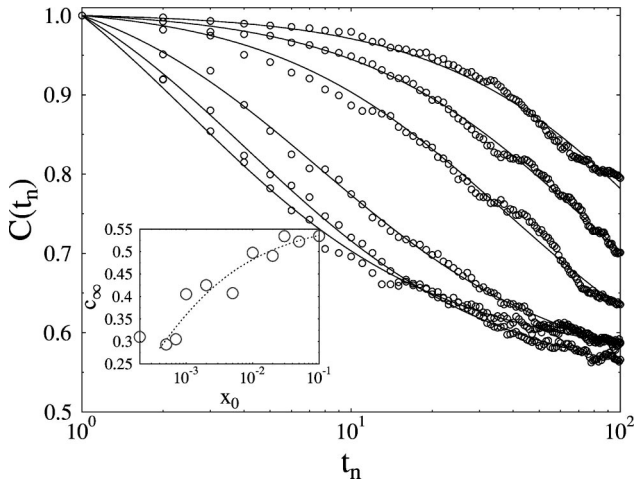

FIG. 10. The density correlation function, $C(t_n)$ from MC data as a function of the logarithm of the tap number t_n, for tapping series with vibrations of amplitude $x_0=2.0\times10^{-4}$,5.0×10^{-4},2.0×10^{-3},5.0×10^{-3}, 1.0×10^{-2},2.0×10^{-2} (from top to bottom) and duration $\tau=37$ (the same as Fig. 1). The continuous curves are inverse logarithmic fits. Inset: Asymptotic value c_∞ of the density correlation function $C(t_n)$, as a function of the vibration amplitude x_0.

In summary, the time correlation function $C(t_n)$ also shows the logarithmic behavior found for the density $\rho(t_n)$ and, consistently, its power spectrum S_C, has the same power law behavior as for $S_\rho(\omega)$.

IV. CONCLUSIONS

In conclusion, our study of density fluctuations in the present microscopic lattice model of vibrated granular media presents a detailed picture of the phenomenon. We found that density fluctuations are of the same order of the measured average values and of the higher order cumulant. They all follow the same kind of inverse logarithmic dynamics in the presence of vibration, as experimentally discovered in the compaction of real granular media undergoing a sequence of taps [7]. As in the proximity of critical points, we typically find power law behaviors in the limit of small vibration amplitudes or durations. For what concerns the power spectrum of density relaxations we observed, for low amplitude tapping sequences, several regions. In particular, at low amplitudes, a wide region with a nontrivial power law appears between a low frequency zone with almost constant behavior and a more usual high frequency region originated by a short time exponential-like relaxation. We also observed a crossover region in vibrations amplitude (approximately located between the amplitudes x_1^* and x_2^*), where the quantitative behavior of the above described laws changes. It is important to note that, being density relaxation logarithmic, our results may not apply in the real asymptotic regime, which also with experiments may be not easily accessible. We have compared our results with experimental measures from Ref. [7], finding substantial agreement, and predictions about the detailed behaviors found here are left for future experimental investigations.

The key feature of the model consists of taking into account the role played in granular media by disorder and geometric frustration in the motion and packing of grains. Intriguing are the connections that appeared with other materials in which geometrical disorder and frustration play a crucial role as glassy systems [13,22,14]. As a matter of fact, some phenomenological theories developed to explain dynamic behaviors in granular media [8,19,14,15], are close in spirit to some approaches developed in the context of the glass transition [25].

ACKNOWLEDGMENTS

The authors are grateful to J.B. Knight and H.M. Jaeger for sending their experimental data, and M.N. thanks J. Rajchenbach for useful discussions. The work was partially supported by TMR Network Contract No. ERBFMRXCT980183 and MURST (Grant No. PRIN-97).

[1] H.M. Jaeger and S.R. Nagel, Science **255**, 1523 (1992); H.M. Jaeger, S.R. Nagel, and R.P. Behringer, Photochem. Photobiol. **49**, 32 (1996); Rev. Mod. Phys. **68**, 1259 (1996).

[2] *Disorder and Granular Media*, edited by D. Bideau and A. Hansen (North-Holland, Amsterdam, 1993); *Physics of Dry Granular Media*, edited by H.J. Herrmann *et al*. (Kluwer Academic, Dordrecht, 1998).

[3] C.-h. Liu, S.R. Nagel, D.A. Schecter, S.N. Coppersmith, S. Majumdar, O. Narayan, and T.A. Witten, Science **269**, 513 (1995).

[4] B. Miller, C. O'Hern, and R.P. Behringer, Phys. Rev. Lett. **77**, 3110 (1996).

[5] G.W. Baxter, R. Leone, and R.P. Behringer, Europhys. Lett. **21**, 569 (1993).

[6] A. Ngadi, J. Rajchenbach, E. Clement, and J. Duran (unpublished).

[7] J.B. Knight, C.G. Fandrich, C. Ning Lau, H.M. Jaeger, and S.R. Nagel, Phys. Rev. E **51**, 3957 (1995).

[8] E. Ben-Naim, J.B. Knight, and E.R. Nowak (unpublished).

[9] E.R. Nowak, J.B. Knight, M. Povinelli, H.M. Jaeger, and S.R. Nagel, Powder Technol. **94**, 79 (1997).

[10] G.W. Baxter, R.P. Behringer, T. Fagert, G.A. Johnson, Phys. Rev. Lett. **62**, 2825 (1989).

[11] J. Andrade, C. Trevino, and A. Medina, Phys. Lett. A **223**, 105 (1996).

[12] S. Horikawa, A. Nakahara, T. Nakayama, and M. Matsushita, J. Phys. Soc. Jpn. **6**, 1870 (1995).

[13] S.F. Edwards, J. Stat. Phys. **62**, 889 (1991); A Mehta and S.F. Edwards, Physica A **157**, 1091 (1989).

[14] T. Boutreux and P.G. de Gennes, Physica A **244**, 59 (1997).

[15] H. Hayakawa and D.C. Hong, Phys. Rev. Lett. **78**, 916 (1999).

[16] A. Rosato, K.J. Strandburg, F. Prinz, and R.H. Swendsen, Phys. Rev. Lett. **58**, 1038 (1987).

[17] T.A.J. Duke, G.C. Barker, and A. Mehta, Europhys. Lett. **13**,

19 (1990); A. Mehta and G.C. Barker, Phys. Rev. Lett. **67**, 394 (1991).

[18] R. Jullien, P. Meakin, and A. Pavlovitch, Phys. Rev. Lett. **69**, 640 (1992).

[19] M. Nicodemi, A. Coniglio, and H.J. Herrmann, Phys. Rev. E **55**, 3962 (1997); Physica A **240**, 405 (1997); J. Phys. A **30**, L379 (1997).

[20] E. Caglioti, H.J. Herrmann, V. Loreto, and M. Nicodemi, Phys. Rev. Lett. **79**, 1575 (1997); M. Nicodemi, Phys. Rev. Lett. (to be published); e-print cond-mat/980346.

[21] M. Nicodemi, J. Phys. I **7**, 1358 (1997).

[22] M. Nicodemi and A. Coniglio, J. Phys. A **30**, L187 (1997); Phys. Rev. E **56**, R39 (1997).

[23] J. Arenzon, M. Nicodemi, and M. Sellitto, J. Phys. I **6**, 1143 (1996).

[24] K. Binder and A.P. Young, Rev. Mod. Phys. **58**, 801 (1986).

[25] G. Adam and J.H. Gibbs, J. Chem. Phys. **43**, 139 (1965).